The Pennsylvania State University
The Graduate School

ATOMIC-SCALE STUDIES OF MOLECULES ON PALLADIUM{111} SURFACE

A Thesis in
Chemistry
by
Rong Zhang

Submitted in Partial Fulfillment
of the Requirements
for the Degree of

Master of Science

May 2008

The thesis of Rong Zhang was reviewed and approved* by the following:

Paul S. Weiss
Distinguished Professor of Chemistry and Physics
Thesis Advisor

Nicholas Winograd
Evan Pugh Professor of Chemistry

A. Welford Castleman, Jr.
Evan Pugh Professor of Chemistry and Physics
Eberly Distinguished Chair in Science

Ayusman Sen
Professor of Chemistry
Head of the Department of Chemistry

*Signatures are on file in the Graduate School.

Abstract

We use a low-temperature scanning tunneling microscope (STM) to conduct an atomic-scale study of thiophene on Pd{111} at 4 K. In one set of experiments, we characterized the Pd{111} single crystal. Two distinct features of subsurface impurities in a normally clean Pd are resolved under topographic images. One is ascribed to S, and the other to either C or O. The vibrational spectrum of the Pd substrate lattice was measured by inelastic electron tunneling spectroscopy with the STM. We find that the vibrational energy of the Pd surface phonon is consistent with previous experimental results and theoretical predictions.

In another set of experiments, we investigated the system of thiophene adsorbed on Pd{111} at 4 K. Thiophene was found preferentially bound to the upper step edges of Pd substrate due to a combination of molecule-substrate interactions and intermolecular attractive dipole-dipole interactions. By resolving the underlying substrate lattice in topography, we are able to determine the adsorption sites and orientations of thiophene molecules on Pd.

We also use the STM as an operative tool to study molecular motions induced by tunneling electrons. We believe that tunneling-electron-induced molecular motions (rotation, translation, dissociation) involve the inelastic electron scattering and relaxation of C-H stretch vibrations to lower energy modes of the molecules that leads to excitation of other degrees of freedom in thiophene. The vibrational relaxation of a single molecule was monitored by time-dependent changes in the current level.

Table of Contents

List of Figures

Acknowledgments

It is a pleasure to thank the many people who made this thesis possible.

I would like to begin by thanking Professor Paul S. Weiss for giving me the opportunity to work in his lab. I am grateful to my advisor for his understanding, encouragement and personal guidance during my graduate career. His scientific perspective and inspiration have been of great value for me. I would also like to thank my thesis committee, Professors Nicholas Winograd, A. Welford Castleman, and Roy Willis, for their scientific insights and advice.

I am indebted to many Weiss group members for providing a stimulating and fun environment in which to learn and grow. I would like to thank Adam Kurland, Sanjini Nanayakkara, Luis Fernández-Torres, Patric Han, and Meaghan Blake, who have been consistently giving me helpful advice whenever I need it. I would also like to thank my group colleagues who have helped me prepare my second year seminar and grilled me before my oral comprehensive exam. Working in the Weiss group has been a wonderful experience to me.

I especially wish to thank my parents, who raised me, supported me, taught me, and loved me. To them I dedicate this thesis. I want to thank my husband Andrey, who has always been with me no matter how dubious my decisions have been. He always gives me warm encouragement and love in every situation. I believe I owe deepest thanks to all people in my entire family who have supported me since I was born.

I am grateful for the support provided by the National Science Foundation (NSF), U.S. Department of Energy (DOE), Multidisciplinary University Research Initiative (MURI), National Institute of Standards and Technology (NIST), and Petroleum Research Fund (PRF).

Chapter 1

Atomic-Scale Studies of Molecules on Palladium{111} Surface

1.1 Why Low-Temperature Scanning Tunneling Microscopy

The scanning tunneling microscope (STM) has developed into a fascinating technique in almost all fields of surface science since its invention by Binnig and Rohrer [1]. It enables imaging surfaces with atomic resolution, the manipulation of single adsorbates, the monitoring of catalytic surface reactions, the investigation of metastable precursors, and the performance of spectrocopic measurement [2, 3]. It has had an enormous impact on our understanding of the structures and the chemical, physical and electronic properties of surfaces.

In this thesis, all experiments were conducted using a custom-built, ultrastable, extreme-high vacuum, low-temperature STM (XHV LT-STM). The advantage of working under XHV conditions is twofold. First, the XHV environment is necessary for experiments on "clean", well-defined solid-vacuum interfaces, where contamination effects can be neglected. Second, the pressure control of the dosage of molecules into the UHV chamber through a sapphire leak valve is straightforward. Along with XHV STMs, helium-cooled low-temperature STMs have been another important development. Working at 4 K, sample cleanliness is greatly extended

due to the efficiency of cryopumping. Our experience tells us that the sample does not undergo degradation over 10 days while maintained at 4 K. Further, the stability of the tunnel junction is enhanced due to minimal thermal drift. The STM is sufficiently stable to keep the STM tip positioned at a single atomic site for hours or days. Moreover, low temperature narrows the electron distribution of both tip and surface and thus greatly enhances both the imaging and spectroscopic resolutions. Finally, thermally activated diffusion is quenched, making it possible to find single isolated adsorbates and study tunneling-electron-induced molecular motions.

1.2 Thesis Overview

In accomplishing the work presented in this thesis, a low-temperature extreme-high vacuum STM was used to study the chemistry and physics of thiophene molecules on palladium surfaces at the atomic level. We first characterized the Pd{111} single crystal by topographic imaging and inelastic electron tunneling spectroscopy (Chapter 2). We assigned two distinct features to two types of subsurface impurities by their contrast under topography. We also determined the vibrational energy of Pd lattice phonons by STM-IETS. In Chapter 3, the adsorption of thiophene on Pd{111} was probed. The role that step edges play in directing molecular adsorption and orientation was investigated. We found that thiophene molecules preferred to bind to the upper step edges while they showed no apparent preference to any of the three binding sites (on-top, hollow and bridge sites) on terraces. Chapter 4 described the ability of using STM to manipulate single molecules on surfaces. Molecular rotation, translation and bond dissociation were observed. The mechanism of these tunneling electron induced molecular motions were speculated to involve inelastic electron tunneling and vibrational relaxation. In Chapter 5 the conclusions from the individual chapters were reviewed and future experimental directions were outlined.

Chapter 2

Characterization of Palladium{111} at 4 K Using Scanning Tunneling Microscopy and Spectroscopy

2.1 Introduction

The motivation for studying the palladium surface is to gain a fundamental understanding of the critical role this substrate plays in catalytic processes, particularly in the processes where palladium is used to catalyze hydrogenation and dehydrogenation reactions. It is known that hydrogen can occupy subsurface sites that are stable absorption sites below the top-most surface layer of Pd atoms. These sites are suggested to be an important link between strongly chemisorbed surface hydrogen and the more weakly bound hydrogen absorbed in the bulk [4]. Several important chemical reactions are thought to involve subsurface hydrogen in Pd, such as hydrogenation of furan [5], hydrodesulfurization of thiophene [6], and alkene hydrogenation by Pd nanoparticles [7]. For the first time, Sykes *et al.* have been able to create this species of subsurface hydride of Pd for direct observation via an inelastic excitation mechanism using the STM [8]. Therefore, characterizing the Pd surface is an important step in understanding the catalytic properties of Pd.

Active sites at which surface reactions occur make key contributions to catalytic processes. The identification of active sites has been an important and long-standing goal of surface science. In many instances, it has been demonstrated

that chemical reactions occur preferentially at defects [9] and monatomic steps [10]. For crystalline surfaces, one type of defects is impurities. Impurities can alter the structure and reactivity of surfaces. An isolated impurity adsorbed on a metal surface modifies the surrounding electronic levels of the metal, both by the shift of bonding geometry with respect to other substrate atoms and by enhancing or diminishing the ability of the surface to bind adsorbates and catalyze reactions. Impurity atoms can also accumulate within and beneath the surface layer [11]. Just as surface impurities, subsurface impurities are expected to perturb the local geometry and electronic structure of the host substrate. Because the STM is extremely sensitive to impurities near surfaces, we are able to distinguish two distinct impurity species beneath the Pd{111} surface by their image contrast.

In this chapter, we will show topographic STM images of a nominally clean Pd{111} surface with resolved features of subsurface impurities and spectroscopy of Pd surface vibrations.

2.2 Sample Preparation

Scanning Tunneling Microscopy. The experiments presented in this chapter, as well as throughout this thesis, have been conducted using a custom-built, low-temperature, ultrastable, extremely high vacuum STM that has been described in detail elsewhere [12]. All STM topographic images have been recorded at 4 K in constant-current mode with a mechanically cut Pt/Ir (85%/15%) tip. All biases in the STM images are referenced to the sample bias.

Inelastic electron-tunneling spectroscopy has been acquired utilizing a lock-in amplifier (model SR830, Stanford Research Systems) to monitor the current's second harmonic (d^2I/dV^2) directly with an AC amplitude of 4 mV (rms) at 1000 Hz modulation. Each STM-IETS spectrum was acquired at a single point on a surface. This was done by holding the STM tip at a constant distance (feedback loop is blanked) from the sample over the point of interest and then sweeping the bias voltage while recording the tunneling current. Since the feedback loop is open, the tip will not try to compensate for the changes in current by adjusting the tip-sample distance.

Palladium Crystal Preparation. Pd{111} single crystal surface (MaTecK,

Juelich, Germany) was cleaned by repeated cycles of Ar^+ sputtering (1000 eV, $I_{\text{sample}} = 5\ \mu$A, 873 K for 15 min), followed by oxygen treatment (873 K, 1.0×10^{-5} torr O_2 backfill for 5 min; 1 torr = 133 Pa) and annealing in vacuum (1100 K for 10 min). Pd cleaniness was assessed with STM as described in the following sections, and we typically observed <0.01% surface impurities and <1% subsurface impurities.

2.3 Scanning Tunneling Microscopy and Spectroscopy of Pd{111}

2.3.1 Microscopy of Pd{111} and Its Subsurface Defects

Sulfur and carbon are two common Pd bulk contaminations. Initial removal of bulk contamination can be achieved by repeated cycles of sputtering with 1 keV Ar^+ and reaction with oxygen followed by annealing to 1100 K. It is useful to distinguish impurities bound externally to the surface from those incorporated into the few outermost layers of the crystal. The former category includes foreign atoms and molecules adsorbed from the gas phase, as well as bulk impurities that thermally segregate to the surface. Cleaning by sputtering and exposure to reactive gases (oxygen treatment is used in our sample preparation) under ultra-high vacuum conditions is usually sufficient to remove such surface contamination temporarily. Impurity atoms can also accumulate within and beneath the surface layer. Impurities in such sites can be quite stable, with significant energy barriers either to segregate onto the surface or to migrate deeper into the bulk. As a result, small quantities of impurity atoms may remain in subsurface sites. Subsurface impurities are expected to perturb the local geometry and electronic structure of the surface. To the extent that the perturbations reach the surface layer atoms, the reactivity of the surface may be affected.

Figure 2.1A shows an STM image of Pd{111} with both surface-bound and subsurface impurities. The surface-bound impurities (denoted with the red right-pointing arrow) are assigned as atomic oxygen resulting from thermal dissociation of oxygen in the sample cleaning procedure. The appearance of atomic oxygen clusters on Pd{111} in our STM images as protrusions is consistent with the study

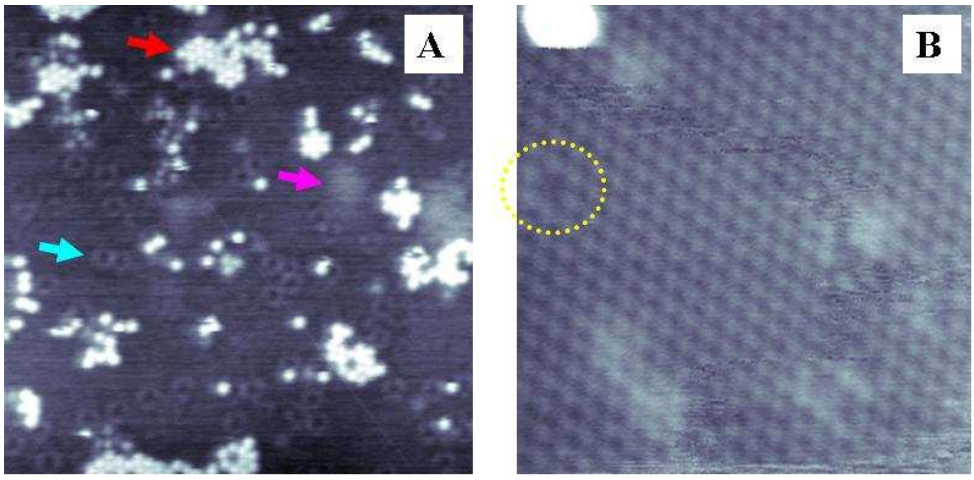

Figure 2.1. Pd {111} surface. (A) STM image ($V_{\text{sample}} = 500$ mV, $I_{\text{tunnel}} = 175$ pA) of a 325 Å×325 Å region of a Pd{111} surface. Surface-bound impurities are denoted by the red right-pointing arrow. Two distinct subsurface impurity features are observed and highlighted with a green arrow, assigned as S, and a pink arrow, assigned as C or O. (B) STM image ($V_{\text{sample}} = 40$ mV, $I_{\text{tunnel}} = 350$ pA) of a 65 Å×65 Å region of clean Pd surface resolving the Pd 1×1 lattice structure. A point defect is highlighted by a yellow circle. The subsurface impurities that appear as protrusions are ascribed to either C or O.

of Rose and co-workers [13]. Two distinct types of subsurface features are also visible in Figure 2.1A, denoted by green and pink arrows. Subsurface impurities are ubiquitous in STM studies of Pd single crystals, and have been characterized by Salmeron and co-workers [14]. The subsurface feature that appears in Figure 2.1A as a depression surrounded by a higher contrast ring (highlighted by green arrow) is ascribed to S, as assigned by Salmeron and co-workers [14]. The subsurface features that appear as protrusions (highlighted by the pink arrow) is ascribed to either C or O; these are difficult to discern from one another. A normally clean Pd surface with <1% subsurface impurities can be obtained through additional cycles of sample treatment. A representative STM image of a clean Pd surface with atomic resolution (Figure 2.1B) shows the hexagonal arrangement of the Pd atoms, a point defect of a Pd atom vacancy and a trace subsurface impurities.

These subsurface species generally have important effects on the electronic, geometric, and chemical properties of the metal surface. Sykes *et al.* observed the effects of Pd subsurface hydride formation in Pd{111} on surface deformation

and charge and on adsorbed hydrogen on the surface [8]. Surface hydrogen atoms are observed to segregate away from the area where subsurface hydrogen causes topographic and electronic perturbations in the Pd top layer. Another STM experiment by Gsell *et al.* shows that small lattice distortions can modify the reactivity of the surface [15]. Strain induced on the nanometer length scale can locally affect the binding energy of adsorbates. In their experiment, bubbles of argon trapped beneath the surface of Ru(0001) caused outward buckling of the surface layer, resulting in expansion in the intralayer spacing to which adsorbed oxygen and carbon monoxide were attracted [15].

2.3.2 Inelastic Electron Tunneling Spectroscopy of Pd{111}

In addition to topographic imaging of surfaces, STM also provides the opportunity to separate the contributions of electronic and geometric structure by using scanning tunneling spectroscopy (STS). The STS technique, first used by Binnig *et al.* [16], involves superimposing a small high-frequency sinusoidal AC modulation voltage on top of the constant DC bias between the sample and tip. Simultaneously with the sample topography, the tunneling conductance $\mathrm{d}I/\mathrm{d}V$ at selected locations of the image or over extended 2-D arrays is measured with a lock-in amplifier. Plots of the conductance $\mathrm{d}I/\mathrm{d}V$ vs. V provide quantitative spectroscopic information of the electronic density of states (occupied and empty) at these locations with atomic resolution. The method has been very useful for characterization of semiconductors [17] and of metals [18-20]. The surface states on several bare surfaces, such as Cu, Ag, and Au, were investigated [18, 19], and it was possible to detect electronic states of adsorbed transition metal atoms [20]. In contrast to noble metals, however, the corresponding surface states on Pd(111) are unoccupied and far above the Fermi energy E_F (1.3 eV above E_F) [21], making it difficult to characterize the surface states of palladium and to study their interactions with defects on a local scale by STS.

Another modulation technique to characterize surfaces and particularly single adsorbates is vibrational spectroscopy. It had been expected that this could be achieved by STM in the same way as with traditional inelastic electron tunneling

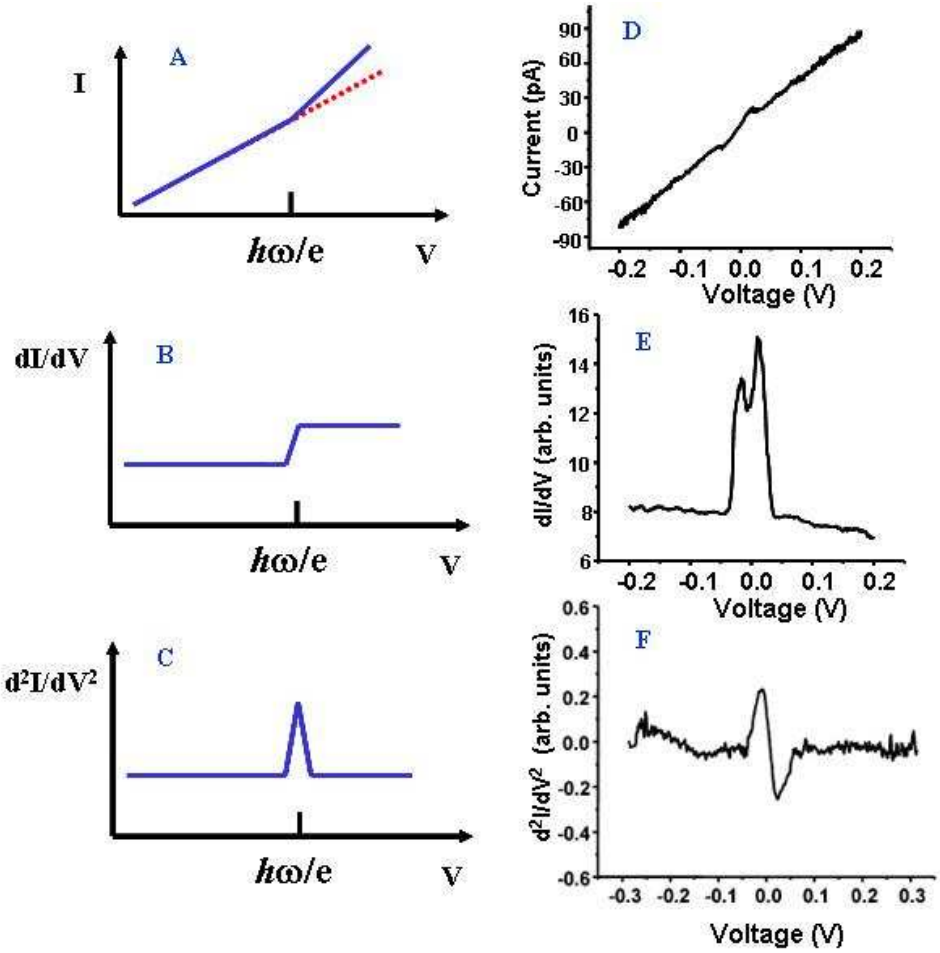

Figure 2.2. (A)-(C) Schematic showing the emergence of inelastic tunneling at the threshold ($V = \hbar\omega/e$) for vibrational excitation. In STM-IETS, when sample bias is increased and crosses the threshold for the excitation of a vibrational mode, the opening of the inelastic electron tunneling channel is accompanied by a slope change in the $I-V$ curve (A). This change is more clearly apparent from (d^2I/dV^2) (C). (D)-(F) Spectra of Pd{111} acquired by E. C. H. Sykes and L. C. Fernández-Torres using the same STM on which the work in this thesis was done. (F) illustrates the symmetry of the Pd phonon features with respect to 0 V bias at ± 0.02 V.

spectroscopy (IETS) [22], which is performed with planar solid tunneling junctions. In IETS, inelastic excitations of vibrations appear as peaks in the second derivative of the tunneling current with respect to the sample bias (Figure 2.2, A-C). Recording (d^2I/dV^2) vs V during scanning of the surface with the STM by selecting specific points could, therefore, provide locally resolved vibrational spectra of substrate lattice or adsorbed molecules. From the characteristic vibrational

energies, chemical identification of molecular species in the tunneling junction is possible [3]. However, the selection rules and excitation mechanism of STM-IETS have not yet been fully understood.

We have performed STM-IETS on bare Pd{111}. Figure 2.2F displays the IETS spectra for bare Pd{111}, which contains features at $\pm 0.02\ V$. Experimentally, a Pd surface phonon feature has been detected with helium scattering and measured in the range of 0.020 - 0.030 eV [23]. Molecular dynamics simulations have predicted a peak at 0.023 eV resulting from a Pd phonon motion [24]. The feature in Figure 2.2F corroborates these values, and has been assigned as a Pd phonon motion. Surface phonons are quanta of lattice vibrations of atoms near the surface and are important in surface physics due to several phonon-related phenomena, such as thin-film reconstructions driven by electron-phonon coupling [25], and size-dependent frequency shifts and broadening of the surface phonon modes for quantum dots [26]. In catalytic reactions, studying surface phonons may provide information about the substrate lattice relaxation and distance change between adsorbates and surface atoms, giving insight on phonon-induced surface change of reactivity [27].

It must be recognized that inelastic tunneling effects are small (the conductance changes by only a few percent), and so demand an extremely stable tunneling gap. To allow averaging of spectra, thermal drift and adsorbate mobility (in the case of adsorbate-metal system) must be minimal, as discussed earlier. That is why low-temperature instruments are necessary for such stringent stability requirements.

2.4 Conclusions

To characterize the Pd{111} surface, we have produced clean Pd surfaces by repeated sputtering/annealing cycles and observed two distinct subsurface impurities features, one assigned to S and the other assigned to either C or O. We have also demonstrated the advantage of STM in recording the vibrational spectra of Pd surface phonons using STM-IETS.

Chapter 3

Adsorption and Interaction of Thiophene on Pd{111}

3.1 Introduction

3.1.1 Motivation

Desulfurization of sulfur compounds, particularly aromatic molecules contained in petrolem fuel, is a catalytically important process due to the deleterious effects of S in the deactivation of refinement catalysts, corrosion of engine parts, and SOx emission. As a model system of the reaction, the adsorption of thiophene (C_4H_4S) on metal surfaces has been studied extensively [10, 28, 29, 30, 31]. Palladium is considered quite important for such catalytic reactions because (1) as one of the late transition metals, it has a high electronegativity that destabilizes aromatic rings by charge transfer from the metal bands to the thiophene antibonding π^* orbital; (2) the Pd metal is well-known as catalyst for hydrogenation and desulfurization of unsaturated and heteroatom-containing species [32]. However, there is currently little molecular understanding of the interaction between the reagent thiophene and the catalytic substrate palladium. Thus, in order to gain a fundamental understanding of such catalytic processes, the study of thiophene on Pd single crystal at atomic level is necessary.

3.1.2 Prior STM Experimental and Theoretical Results

Hamers and co-workers imaged rotational orientation of thiophene derivatives on a Ag{111} surface at 120 K. [31]. Thiophene, 2,5-dimethylthiophene and 2,2'-bithiophene, were dosed onto vacuum-evaporated Ag{111} surface. All three molecules preferentially bind at step edges. Images of dimethylthiophene and bithiophene molecules show an elongated structure while thiophene appears near-circular. The long axis of dimethylthiophene molecular images is oriented perpendicular to the step edges while that of bithiophene is parallel. Chen *et al.* proposed that the rotational orientation of dimethylthiophene at Ag(111) step edges is due to intermolecular dipole-dipole interactions [33]. They also observed that at high coverages a phase transition occurs from the thiophene molecules lying with their molecular plane parallel to the surface to a tilted geometry. Kushmerick *et al.* studied the adsorption of thiophene on Ni{110} and proposed a four-fold binding geometry [10]. Chiang and her group calculated the STM images of isolated thiophene on Pd{111} as a function of adsorption sites [34].

In this chapter, we will discuss our study of thiophene on Pd{111} in terms of the Smoluchowski effect, thiophene adsorption sites and orientations on Pd surface step edges as well as terraces and interactions between the adsorbates and substrate.

3.2 Experimental

The Pd{111} single crystal cleaning methodology has been described in Chapter 2. Neat thiophene (99.9% purity) was obtained from Sigma Aldrich and was further purified by cycles of freeze/pump/thaw prior to introduction to the UHV chamber. Purity of the gas-phase thiophene was verified by a quadrupole mass spectrometer. The Pd{111} substrate was exposed to thiophene by backfilling the main chamber to 1×10^{-5} Torr of thiophene vapor for 40 seconds via a leak valve shortly after the crystal was transferred to 4 K STM chamber.

All STM images were acquired in constant-current mode at 4 K and are presented unfiltered. Differential conductance images were acquired using a lock-in amplifier (LIA) (model SR850, Stanford Research Systems) by phase-sensitive de-

tection of the first harmonic of the tunneling current with respect to the bias, which corresponds to the differential conductance of the tunneling current. The differential conductance was acquired via the LIA by modulating the bias voltage with an ac amplitude of 4 mV (V_{rms}), 1000 Hz and acquired with a 10 ms time constant.

3.3 Results and Discussion

3.3.1 Adsorption at Step Edges

Figure 3.1A shows an STM image of 0.1 monolayers (ML) of thiophene adsorbed on Pd{111}. The crystal was dosed shortly after it had been transferred from room temperature to the 4 K stage on the STM (*i.e.*, before it was completely cooled down). That allows thiophene molecules to diffuse across the surface before reaching their low-energy adsorption sites such as at steps and surface defects. The features running horizontally in the image are monatomic steps on the Pd substrate; the protrusions are thiophene molecules adsorbed mostly along the upper step edges. Nucleophilic molecules adsorb preferentially on the top of surface step edge as has been observed in several systems, such as furan on vicinal Pd{111} [35], benzene on Au{111} [36], and thiophene on Ag{111} [31]. The factor influencing the adsorption at step edges is the Smoluchowski electron-smoothing effect [37], in which electrons "spill over" at the step edge, leaving the upper step edge slightly depleted of electrons and the lower step edge slightly enriched. The net result of this electron redistribution is the formation of an in-plane surface dipole oriented perpendicular to the step edge, with its positive end on the upper terrace and its negative end on the lower terrace.

Thiophene has a permanent dipole moment of 0.5 Debye [38], with the negative charge located on the sulfur lone pair electrons and the positive charge delocalized among the aromatic ring system. To determine the orientation of thiophene at step edges, we discuss further how a molecule with a dipole moment interacts with a step edge. Chen *et al.* proposed two possible interactions [33]. One possibility is for the molecule to orient across the step edge in order to maximize the purely electrostatic, attractive dipole-dipole interaction between the molecule and the

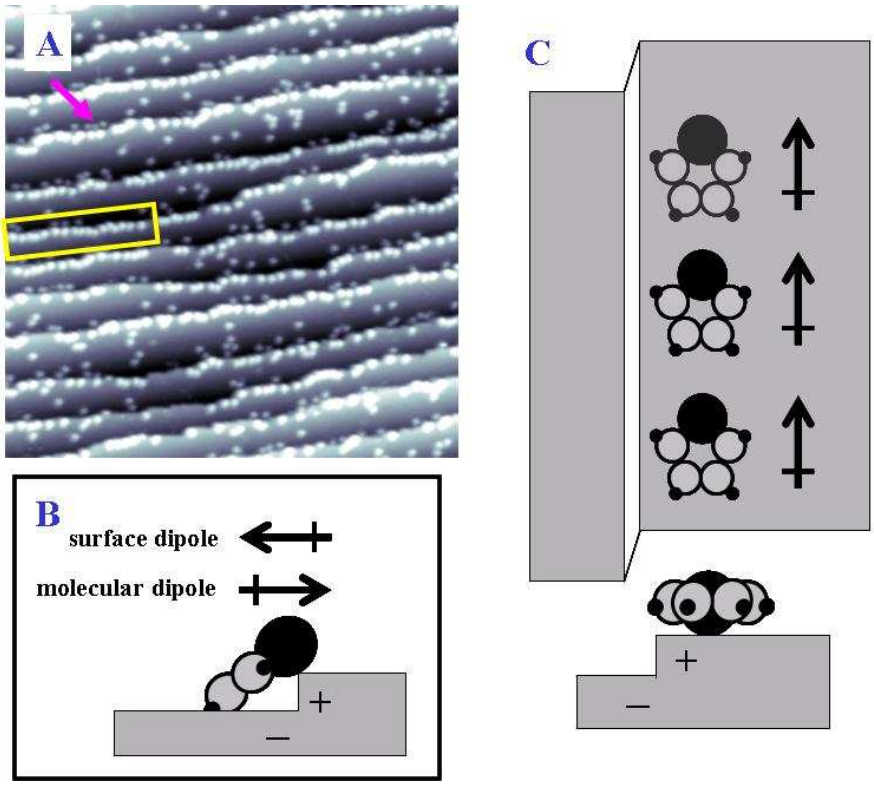

Figure 3.1. STM image (V_{sample} = -0.5 V, I_{tunnel} = 100 pA, 325 Å× 325 Å) of molecular thiophene aligned preferentially along the top of step edges on a Pd{111} surface at 4 K. Thiophene was dosed shortly after the surface was annealed and before the crystal was completely cooled down to 4 K. Noted that some molecules are also adsorbed below step edges (denoted by pink arrow). A segment of step edge is saturated with thiophene molecules (highlighted by yellow box). (B) One possible way (not in our case) for a molecule to interact with a step edge. The orientation of the molecule maximizes the attractive dipole-dipole interactions between itself and the step edge, as described by Chen *et al.* [33]. (C) Proposed orientation of thiophene at step edges. Molecules are aligned at the upper step edge. Intermolecular dipole interactions are attractive.

step edge (Figure 3.1B). In this case, the molecules are expected to bridge across the step edge. Additionally, since all molecules would be oriented in the same direction, the molecular dipoles would all align perpendicular to the step edge, and the intermolecular dipole-dipole interactions would be repulsive, so that molecules adsorbed across the step would repel one another and would not cluster. Contrary to this suggestion, we did not observe molecules bridging the step edge.

A second possibility for molecular orientation is for the molecule-substrate interactions to be dominated by charge transfer between the molecule and the sub-

strate. The positive charge at the upper step edge leads to the creation of a nucleophilic site. If the interaction between the molecule and the substrate depends strongly on charge transfer, then spatially localized bonding at either the upper step edge (for electron-rich molecules) or at the lower step edge (for electron-poor molecules) will result. The STM image in Figure 3.1A indicates that the thiophene molecules lie along the upper step edge. The observation of clustering along the steps also proves that the intermolecular dipolar interactions are attractive. In the step edge region where the molecules have condensed into a linear array (denoted by the yellow box), the separation between thiophene molecules is measured as 6.3±0.5 Å. This value closely approximates 7.0±0.1 Å of the molecular separation at the minimum in the potential energy diagram of two thiophenes held in a coplanar configuration in a head-to-toe geometry calculated using *ab initio* molecular orbital methods [33]. Based on the above discussion, we have determined the rotational orientation of thiophene at the step edge, shown in Figure 3.2C. We believe that the primary interactions for bonding the molecules to the upper step edge are the electron donation from the sulfur lone pair to the positively charged upper step edge and the attractive intermolecular dipole-dipole interactions. However, we could not determine the adsorption sites of thiophene at step edges as we did not resolve the atomic substrate lattice near the steps.

It is not surprising to see some bonding occur at the lower step edge (highlighted by the pink arrow in Figure 3.2A), since empty states originating at the step riser hang out ∼5 Å beyond the step edge, as previously observed in the study of benzene on Cu{111} by Stranick *et al.* [39], and thus offer relatively favorable adsorption sites near the bottom of step edges over terraces. Moreover, at high coverage, substrate-mediated interactions will control the adsorption sites of additional molecules. Stranick *et al.* have shown that the presence of adsorbed benzene molecules at step edges induces perturbations of the surface local density of states (LDOS) near the steps and thus creates favorable adsorption sites for additional molecules [39].

3.3.2 Adsorption on Substrate Terraces

We have obtained simultaneously resolution of the substrate lattice and of the molecule (Figure 3.2A). Thiophene molecules appear as protrusions from the otherwise flat Pd substrate. The thiophene molecule is found to lie flat on the surface at low coverage [40]. This is reasonable since thiophene is a π acceptor and interacts with Pd through the d-π^* back donation. The σ donor character of S lone-pair electrons has little effect on the molecular orientation on the surface. To assign the adsorption sites for the molecules, we highlighted the underlying Pd lattice (Figure 3.2B). It is apparent that some molecules (the highest contrast) are bound to the bridge sites, while others are at either the on-top sites or hollow sites.

As positive sample bias probes the unoccupied states of the sample, we compare the molecular features in our STM image with that of predicted image of unoccupied states of thiophene on Pd calculated by Chiang and her group using extended Hückel molecular orbital theory [34]. The upper left image in Figure 3.2 is an image of the lowest unoccupied molecular orbital (LUMO) for an isolated thiophene. Due to the dipole moment of the thiophene, the LUMO shows high electron density along the carbon backbone. For on-top site bound thiophene, their calculation is able to resolve both the molecule and metal atoms (middle left inset). The feature in the bridge-site image (lower left inset) shows a mixture of the features of the LUMO and of the on-top site.

One common feature for different adsorption sites is that due to its strong electronegativity, the sulfur atom appears less protruding than the carbon ring. Due to resolution limits of the STM, we are unable to resolve the internal structure of the molecule, but the observed overall molecular feature shows excellent qualitative correspondence with the theoretical images. The dim feature near the sulfur allows us to distinguish orientations of thiophene on Pd. Therefore, we are able to assign both adsorption sites and orientations for each molecule in the STM image (right in Figure 3.2).

Figure 3.3 shows the assigned adsorption sites and orientations of all seven molecules. The numerals indicate the rotation angle in degrees, Φ, of sulfur as shown in the inset. Among the seven molecules, we observe that four bound to bridge sites, two to on-top sites, and one to a hollow site. The rotational preference is either 0° or -30° in our observations. Chiang and her group expect

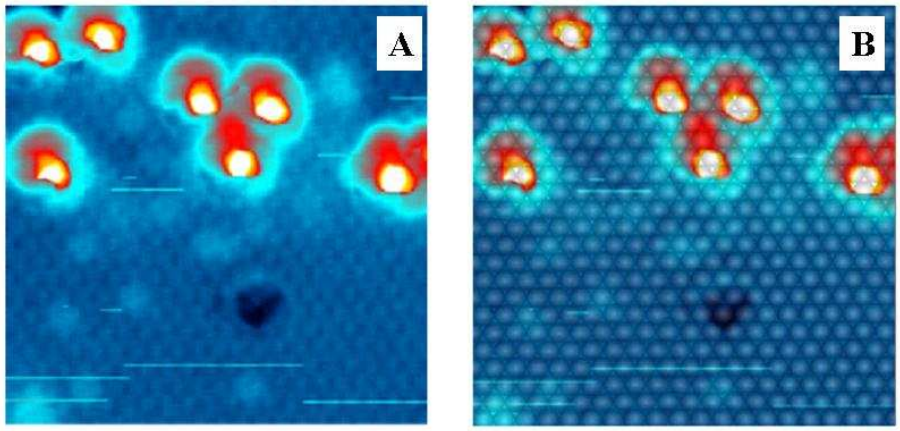

Figure 3.2. STM image of a 60 Å×60 Å area with thiophene molecules at low coverage on Pd{111} at 4 K ($V_{\text{sample}} = 10$ mV, $I_{\text{tunnel}} = 100$ pA). (A) The underlying Pd{111} lattice is resolved and (B) is highlighted to assign adsorption sites and orientations for the molecules.

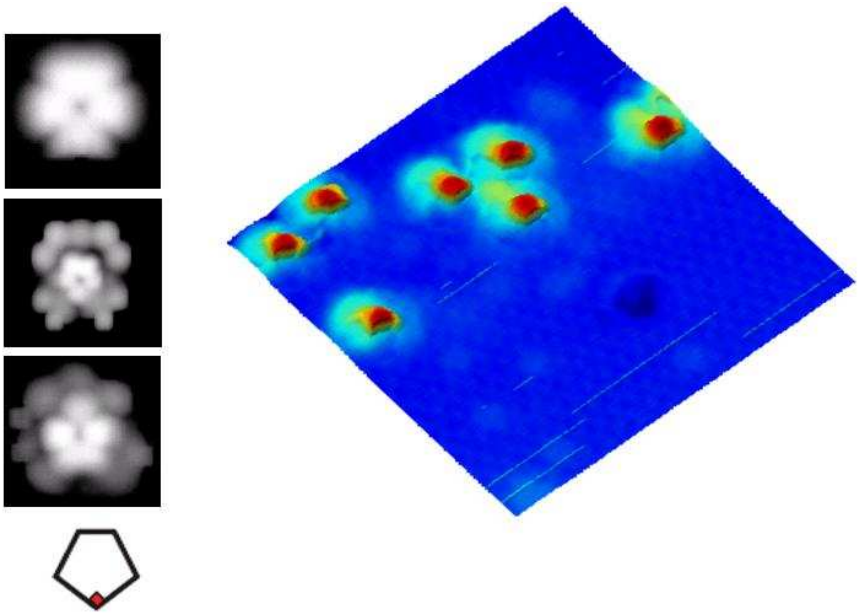

Figure 3.3. Calculated images of unoccupied states of (upper left) isolated thiophene, (middle left) on-top site adsorbed thiophene with resolved metal atoms, and (lower left) bridge site bound thiophene by Chiang *et al.* [34]. In all the calculated images, the sulfur appears with less contrast than the carbon backbone. (Right) Experimental STM image ($V_{\text{sample}} = 10$ mV, $I_{\text{tunnel}} = 100$ pA) of thiophene on Pd. The internal structure in the molecule was not resolved, but the overall feature of the molecule resembles the calculated images. The sulfur atom is assumed to be a relatively low contrast feature under positive sample bias because it is more electronegative than carbon.

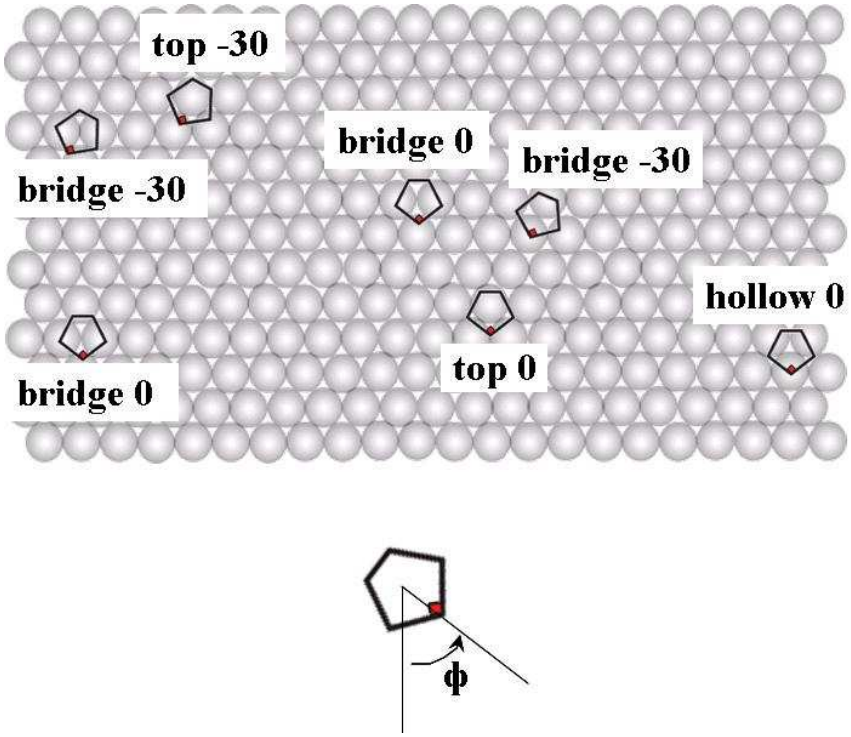

Figure 3.4. Assigned adsorption sites for each thiophene molecule on Pd{111}. The numerals indicate the rotation angle in degrees, Φ, of sulfur as shown in the inset.

the on-top site to be the most probable binding site from their energy calculations, followed by 3-fold hollow site, and then bridge site [34]. For both on-top and hollow sites, 0° rotation is predicted to be the most energetically favorable, while for bridge sites, their binding energy computations find no discernible preference between the 0° and 90° orientations. However, in our experiment, all three binding sites are found possible for thiophene on Pd{111} at 4 K. This is not unusual at low temperature. Sautet and Bocquet calculated STM images of benzene on Pt{111} and found that the most stable adsorption sites were the hollow (Φ=0) and the bridge (Φ=-30) [41], while in earlier experimental STM images at 4 K, Weiss and Eigler were able to obtain three distinct shapes for benzene on Pt{111}, corresponding to three different adsorption sites [42].

3.3.3 Differential Conductance Imaging of Thiophene

Surface defects and adsorbates perturb the electronic structure of the surrounding surface. These perturbations are important as they affect the structure, dynamics

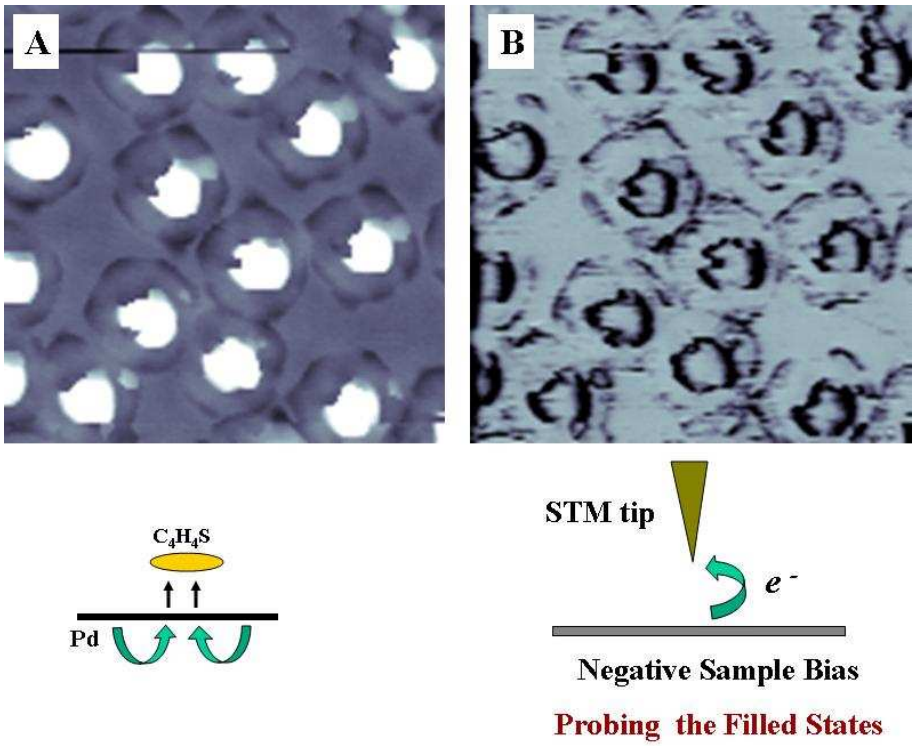

Figure 3.5. (A) Topographic STM image (V_{sample} = -25 mV, I_{tunnel} = 100 pA, 33 Å × 33 Å) and (B) simultaneously obtained differential conductance image of thiophene on Pd{111}. (Bottom left) The interaction between adsorbates and Pd substrate results in charge transfer from the Pd bands to the thiophene π^* orbital, hence depleting the surrounding electron density on the Pd surface and enhancing the local density of empty states. (Bottom right) At negative sample bias, the STM probes the filled states and thiophene appears as protrusion surrounded by depression (bottom right). The effect of adsorbate-substrate interaction on the perturbed surface LDOS is more apparent in the differential conductance image (B) in which the electronic structure is deconvoluted from the geometric structure.

and reactivity of the adsorbates themselves as well as other adsorbates [43]. Spectroscopic measurements, either current-voltage ($I - V$) curves or bias-dependent imaging with STM are a direct way to study the electronic properties of surfaces and adsorbates on surfaces. By inverting the bias polarity applied between the tip and sample, the filled or empty states of the sample can be studied. A negative sample bias probes the occupied states, while a positive sample bias probes the unoccupied states. Differential conductance imaging (dI/dV map at a certain sample bias) also reveals information about the local density of states of the sample.

Topographic images present a convolution of electronic and structural com-

ponents of the surface. By simultaneously recording topographic and differential conductance images, we are able to deconvolute the effects of topography and electronic structure (Figure 3.5). The interaction between thiophene and the Pd substrate results in the charge transfer of 1.1 electrons from the Pd bands to the thiophene π^* orbital [40]. Figure 3.5 bottom illustrates the bias dependent imaging mechanism of adsorbate perturbed local surface. The charge transfer from the Pd d-band to thiophene π^* orbital results in depleted filled states surrounding the adsorbates on the Pd surface (bottom left schematic). Thus, in the case of negative sample bias, the STM probes the filled states and thiophene appears as a protrusion surrounded by depression. The effect of thiophene-Pd interactions on the perturbed electronic structure of the surface is more easily seen in differential conductance images (Figure 3.5B) where the electronic structure is somewhat separated from the topography.

3.4 Conclusions and Future Directions

In this study, we have shown that thiophene molecules are adsorbed at upper step edges with specific orientations. The observed adsorption geometries are determined by a combination of molecule-substrate interactions together with intermolecular attractive dipole-dipole interactions. Atomic resolution of the Pd{111} substrate lattice is obtained with adsorbate features, which qualitatively match calculated STM images. At 4 K, all three binding sites (on-top, hollow and bridge sites) are found possible for thiophene on Pd{111} terraces. We have also demonstrated the advantage of differential conductance imaging in revealing the spatial modulation of the surface LDOS surrounding an adsorbate by separating the electronic structure of surface from the topography. Future experiments using hydrodesulfurization of thiophene on Pd{111} as a model system will be conducted to elucidate the chemistry of subsurface hydride of Pd, a species created for the first time in our group using a 4 K STM [8] and hypothesized to be critical in hydrogenation reactions.

Chapter 4

Single Molecular Motion Induced by Tunneling Electrons

4.1 Introduction

In 1959, Richard Feynman presented a vision of manipulation and control on an atomic scale in his classic lecture "There's Plenty of Room at the Bottom" [44]. In recent years, this vision has been realized. Since its inception, the STM has been further developed from an imaging instrument with atomic resolution to an operative tool. The STM has been used to manipulate and to assemble atoms on surfaces [45]. The tip of the STM can catalyze surface reactions [46]. Electrons tunneling through the electronic states of a molecule adsorbed on a surface also couple to intrinsic molecular motions such as rotation and vibration, leading to the possibility of inducing chemical transformation in the molecule [47, 48]. Inelastic tunneling electrons can also be tuned to induce either bond formation or translation or desorption of individual molecules on surfaces [49, 50].

In this chapter, tunneling electrons are used to induce and to monitor the motions of single molecules, namely, thiophene adsorbed on Pd{111} at 4 K. We precisely positioned the STM tip above the molecule, rotated the molecule with tunneling electrons from the STM tip without perturbing neighboring molecules, and imaged the consequent molecular motion. The precise moment of motion of the molecule studied was monitored as a sudden change in the tunneling current. We will further discuss the mechanism behind the tunneling-electron-induced molecular motion.

4.2 Experimental

The Pd{111} single crystal was cleaned by cycles of Ar^+ ion sputtering and annealing (Section 2.2). All STM images shown were recorded at 4 K in constant-current mode and the bias voltage refers to the sample bias. Thiophene was purified through several freeze-pump-thaw cycles then dosed via a leak valve to the vacuum system. The purity was verified via residual gas analysis by a quadrupole mass spectrometer.

To induce motion of the molecule in the tunneling junction, the feedback mechanism was turned off, the tip was positioned at a chosen point above a molecule, a voltage pulse was applied to the sample, and the time dependence of the tunneling current was recorded during the pulse. The tip remained stationary during the voltage pulse, *i.e.*, the gap distance is held fixed, and the current change is attributed to the molecular rotation or translation underneath the tip.

4.3 Results and Discussion

In this section, we use tunneling electrons from an STM to excite and to induce changes in a molecule. From these changes, detailed properties of the molecule are revealed.

Rotation. After finding an isolated thiophene molecule (Figure 4.1A, denoted by pink arrow), we positioned the STM tip over the center of the molecule. The voltage was then increased to 350 mV, and the tunneling current was recorded. During a 60-second period voltage pulse, we observed a sudden change in the current at $t \sim 40$ s, where t is the time after the initiation of the pulse. We speculate that this current change represents the moment of rotation and each current level corresponds to a rotational orientation of the molecule. The current spikes at $t >$50 s appear each time the molecule rotates underneath the tip. The motion of the molecule, translation coupled with rotation, is evidenced by the streaky feature in the STM image (Figure 4.1C) when the tip was scanned over the molecule.

It should be noted that, in contrast to free rotations for molecules in the gas phase, these single-molecule rotations correspond to hindered rotations where en-

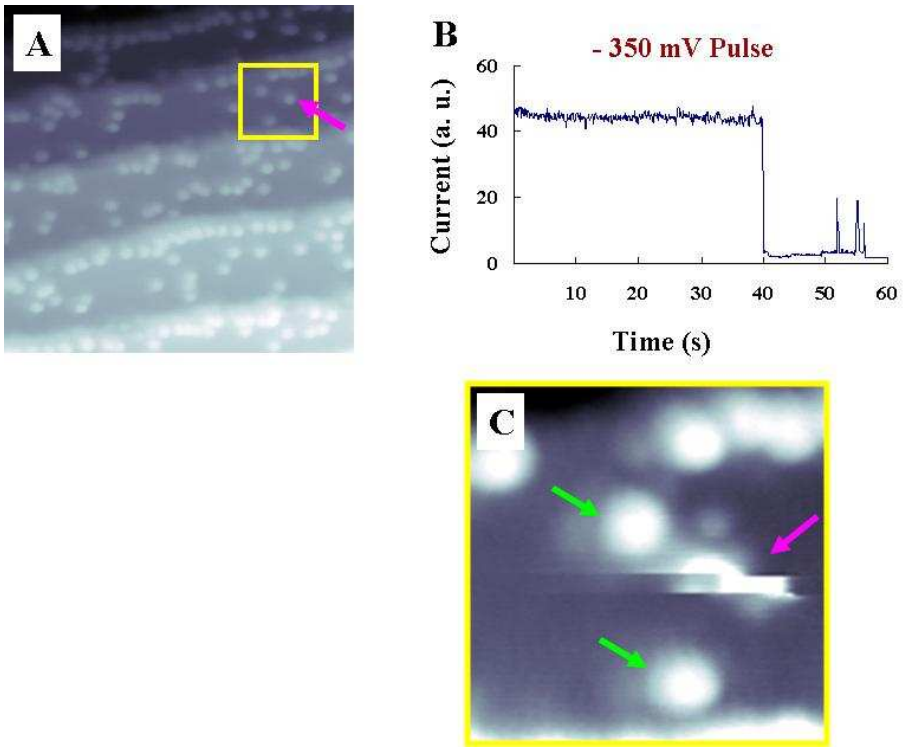

Figure 4.1. Inducing molecular rotation with tunneling electrons. (A) STM image of thiophene adsorbed on Pd (V_{sample} = -150 mV, I_{tunnel} = 100 pA, 162 Å×162 Å). A 350 mV voltage pulse was applied to an isolated molecule on terrace (denoted by pink arrow) for 60 seconds. (B) Current during the 350 mV pulse over the isolated molecule showing the moment of rotation (step at t ∼40 s, where t is the time after the initiation of the pulse). (C) After-pulse image showing the continuous rotation of the stimulated molecule (V_{sample} = -250 mV, I_{tunnel} = 100 pA, 33 Å×33 Å). The same voltage pulse was applied to molecules near the step edge and at the bottom at the step edge (denoted by green arrows). However, no sudden current change or motion was observed for these two molecules.

ergetic barriers between stable sites are crossed in the rotational process. We believe that the mechanism for single-molecule rotation involves inelastic tunneling electron scattering. In each scattering process, energy is transferred to the hindered rotational mode of the molecule. The maximum energy of the tunneling current is given by eV, where e is the charge of a single electron and V is the bias voltage applied to the sample. If eV is greater than the barrier to rotation, E, the barrier can be overcome in one scattering event. If eV is less than the barrier E, the barrier may be overcome in several scattering events, in which each event promotes the molecule to a higher hindered rotational quantum state in a

ladder-climbing fashion [51]. Prior experiments also found that excitation of the adsorbate-substrate vibrational mode enhances the molecular change on surface. For example, the rotation of C_2H_2 on Cu is enhanced with the excitation of C-H stretching vibrational mode at 364 mV pulse [48]. However, the detailed mechanism of the coupling between the rotation of the molecule and the vibrational mode is still uncertain.

In our experiments, we found that when the voltage pulse was reduced from 350 to 300 mV, no rotation was observed for the molecule studied. Although we have not yet conducted such experiments with different tunneling currents, we believe that for a certain voltage pulse, the rotation rate will be current dependent, as the rate of energy transfer from tunneling electrons to the hindered rotational mode of the molecule depends on the amount of electron flow between the molecule and STM tip, *i.e.*, the tunneling current.

When the molecules were adsorbed next to the bottom of or near a step edge such as the ones shown by the green arrows in figure 4.1C, the same voltage pulse (350 mV, 60 seconds) did not induce any motion of these molecules and no jump was observed in the tunneling current. The lack of rotation reveals the importance of local environmental effects.

Translation. We also observed lateral translation of a molecule onto a different adsorption site after the voltage pulse, ascertained by subsequent imaging of the surrounding area (Figure 4.2). The moment of translation is evidenced by a current spike (*e.g.*, at $t \sim$43 s in Figure 4.2B). Such nonthermal diffusion of surface species under electron irradiation was also observed for CO molecules adsorbed on Pd{110} [52] and NH_3 on Cu{100} [50]. These studies reveal that the chance of activating the translational mode depends on the probability of energy transfer from the C-O or N-H stretching vibrational mode into translational mode levels above the molecular diffusion barrier. In the study of CO adsorbed on Pd{110}, Komeda *et al*. found that internal energy transfer via anharmonic coupling between these two modes can be important decay channel for an internal vibration to induce motion of an adsorbed molecule [52]. We believe that the observed lateral translation of thiophene on Pd follows a similar mechanism as the energy of voltage pulse applied (350 mV) is close to the excitation energy of the C-H stretching vibration mode (364 mV).

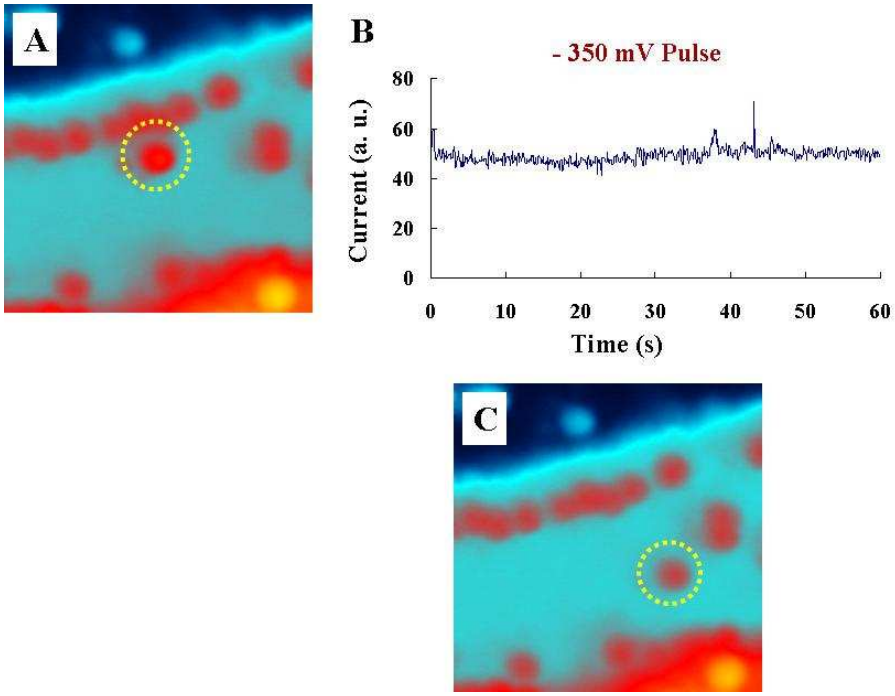

Figure 4.2. Inducing molecular motion with tunneling electrons. STM images (A) before injecting 350 mV electrons over a single molecule (highlighted by yellow circle) and (C) of same area after injecting electrons. (B) Current during a 350 mV pulse showing the moment of translation (spike at t ~45 s). STM imaging condition: V_{sample} = -200 mV, I_{tunnel} = 100 pA, 52 Å×52 Å. A chain formation at the step edge is used as a reference point.

Dissociation. Further electron injection over the molecule studied (circled in Figure 4.2) brought it next to another adsorbate (see Figure 4.3A). As mentioned above, local environmental affects molecular behavior. For example, Stipe *et al.* found that a molecule adsorbed next to a defect (impurity) site quickly returned to a preferred orientation after a voltage pulse [47]. In our experiment, we observed that binding next to another adsorbate hindered tunneling-electron-induced molecular rotation with a 350 mV pulse. It is also possible that the energy transferred from the electron injected to the hindered rotational mode was too small for the molecule to overcome its new rotational barrier. Thus, we increased the pulse to 500 mV and observed a current change at t ~33 s. Subsequent STM imaging showed a feature change of the molecule investigated after the pulse. This feature change from a round protrusion to a two-lobe shape is not due to a tip change, as all the other unprobed adsorbates appear the same as before.

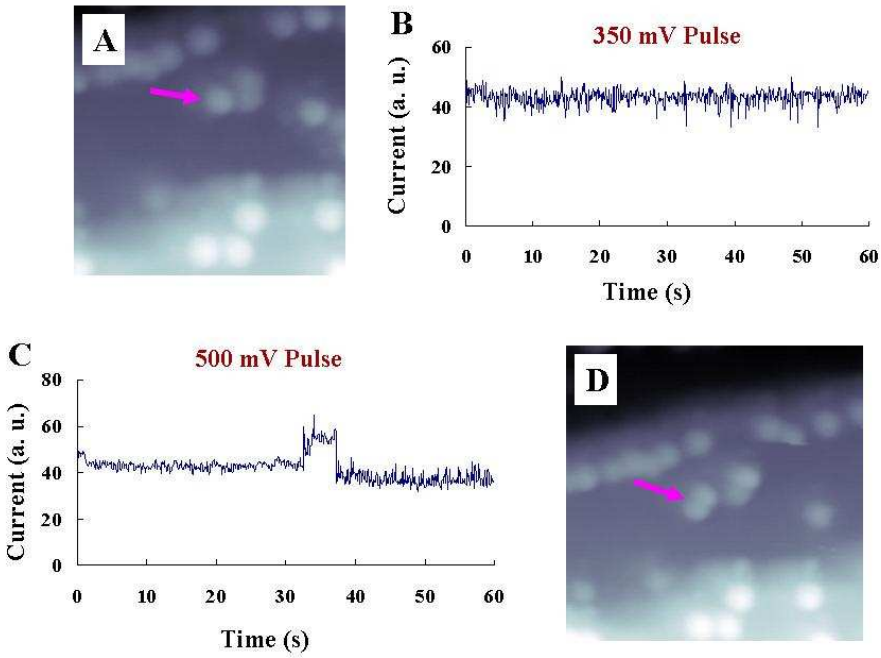

Figure 4.3. A voltage pulse was applied to the molecule, denoted by pink arrow in (A). (B) Current during a 350 mV pulse over the molecule. No current jump was observed during the 60-second pulse. (C) Current during a 500 mV pulse over the molecule, showing a 5 second duration of high level current. (D) STM image of the same area as (A), showing a molecular feature change after the second pulse. STM imaging conditions: $V_{\text{sample}} = 200$ mV, $I_{\text{tunnel}} = 100$ pA.

To probe the internal structure of the molecule and to understand its feature change in STM imaging, we applied a voltage pulse to each of the two lobes. During a 60-second 500 mV pulse, no stepwise current change was recorded when the pulse was applied to the upper lobe, while four current levels were observed when the lower lobe was investigated (Figure 4.4). Due to the different chemistry of the two lobes, we speculate that the molecule underwent a unimolecular reaction such as bond dissociation during electron irradiation, producing two different fragments. To understand this phenomenon further, a full theoretical analysis needs to take into consideration the molecular potential-energy surface, the associated electronic and vibrational excitations, and the coupling of electrons to nuclear motion. Also, STM-IETS could be used to identify reaction products based on their characteristic vibrational spectra.

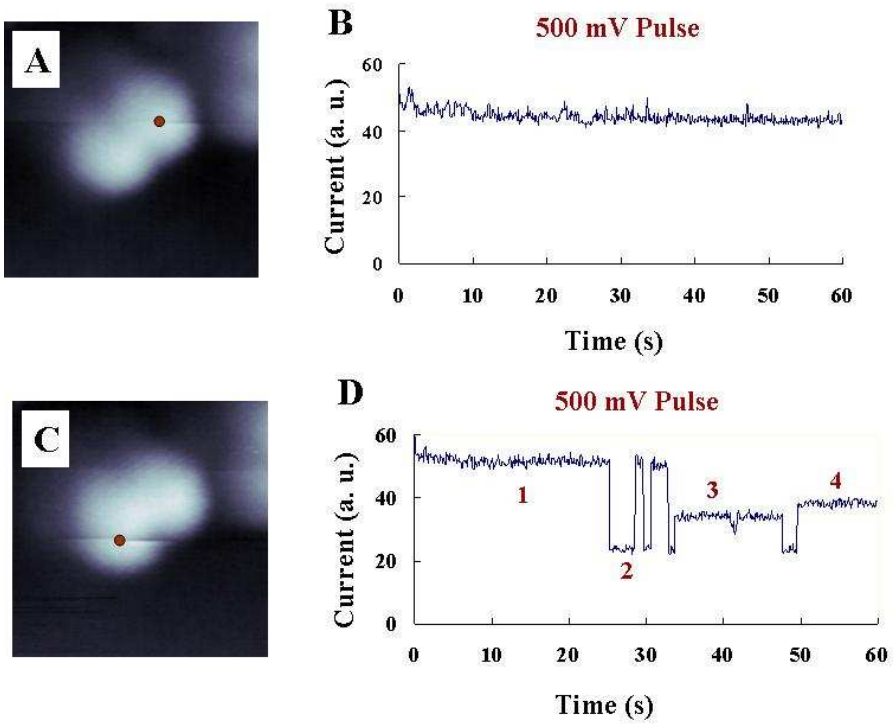

Figure 4.4. Probing the internal structure of a molecule. (A) and (C) STM images of a two-lobe-shaped molecule on Pd. (B) and (D) Current during a 500 mV pulse over one of the two lobes of the molecule, denoted by red dot in (A) and (C). No significant current change was observed in (B) while four levels of current were observed in (D). They may correspond to four orientations of the molecule fragments. STM imaging conditions: $V_{\text{sample}} = 200$ mV, $I_{\text{tunnel}} = 100$ pA, 13 Å×13 Å.

4.4 Conclusions and Future Directions

The excitation of a single molecule has been studied by injecting electrons through the molecule using the STM tip. The relaxation of the high-energy C-H stretch vibration to lower energy modes of the molecule and the substrate leads to excitation of other degrees of freedom in thiophene, such as rotation and diffusion. The vibrational relaxation of a single molecule was monitored by time-dependent changes in the current level. We believe that the mechanism of the tunneling electron induced molecular motions involves inelastic electron tunneling. Further, the induced molecular motions (vibration, rotation, translation) are responsible for inducing nuclear motions. In our last experiment, excitation energy is ultimately converted into dissociation. It remains a challenge to decipher the pathway and

to determine the identity of the reactants, intermediates, and products in a chemical reaction induced by STM. Action spectra (the rate of single molecular motion plotted against sample bias or tunneling current) will be recorded to determine the coupling of electrons to molecular motions.

Chapter 5

Conclusions and Proposed Future Directions

Atomic-scale study of molecules on metal surfaces has been achieved using a low-temperature STM and described in this thesis. Each chapter discusses a unique perspective of the chemistry and physics of molecules on surfaces.

In Chapter 2, we discerned two types of subsurface impurities of Pd{111} by their distinct features and contrasts under topography. We have determined the vibrational energy of the Pd lattice phonons by inelastic electron tunneling spectroscopy. Studying subsurface impurities and substrate phonon will help understand their effects on surface reactivity.

In Chapter 3, we used the adsorption of thiophene on palladium as a model system to gain a molecular understanding of the interaction between reagent and the catalytic substrate Pd. We have determined the effect that step edges have in guiding molecular adsorption and orientation. In future experiments, still using the adsorption of thiophene-on-Pd as a model system, we will elucidate the chemistry of the subsurface hydride of Pd, a species created for the first time in our group using the STM by Sykes *et al.* [8] and hypothesized to be critical in hydrogenation reactions. We will use the ability of STM tip to manipulate the reagents – subsurface hydrogen in and thiophene on Pd{111} in order to drive and to control the hydrogenation and desulfurization of thiophene, probing the reaction mechanism at atomic/molecular level and understanding the high reactivity of subsurface hydrogen.

Finally, we investigated the tunneling-electron-induced molecular motions in Chapter 4. The coupling of electrons to lower energy modes (vibrational and ro-

tational) and nuclear motions of the molecule leads to excitation of degrees of freedom in thiophene, such as rotation, diffusion and dissociation. The probability of such coupling will be quantitatively determined in the future by studying the time dependence of current at various voltages and tunneling currents. The mechanistic understanding of the chemistry induced by tunneling electrons will also involve the theoretical analysis of the excited states of the molecule.

References

[1] G. Binnig, H. Rohrer, C. Gerber, and E. Weibel, 7×7 Reconstruction on Si(111) Resolved in Real Space, *Physical Review Letters* **50**, 120 (1983).

[2] L. Bartels, G. Meyer, and K. H. Rieder, Basic Steps of Lateral Manipulation of Single Atoms and Diatomic Clusters with a Scanning Tunneling Microscope Tip, *Physical Review Letters* **79**, 697 (1997).

[3] B. C. Stipe, M. A. Rezaei, and W. Ho, Localization of Inelastic Tunneling and the Determination of Atomic-Scale Structure with Chemical Specificity, *Physical Review Letters* **82**, 1724 (1999).

[4] B. D. Kay, C. H. F. Peden, and D. W. Goodman, Kinetics of Hydrogen Absorption by Pd(110), *Physical Review B* **34**, 817, (1986).

[5] M. Shirai and M. Arai, Hydrogenation of Furan with Hydrogen Atoms Permeating through a Palladium Membrane, *Langmuir* **15**, 1577 (1999).

[6] M. Shirai, Y. Pu, M. Arai, and Y. Nishiyama, Reactivity of Permeating Hydrogen with Thiophene on a Palladium Membrane, *Applied Surface Science* **126**, 99 (1998).

[7] A. M. Doyle, S. K. Shaikhutdinov, S. D. Jackson, and H.-J. Freund, Hydrogenation on Metal Surfaces: Why are Nanoparticles More Active than Single Crystals? *Angewandte Chemie International Edition* **42**, 5240 (2003).

[8] E. C. H. Sykes, L. C. Fernández-Torres, S. U. Nanayakkara, B. A. Mantooth, R. M. Nevin, and P. S. Weiss, Observation and Manipulation of Subsurface Hydride in Pd{111} and Its Effect on Surface Chemical, Physical, and Electronic Properties, *Proceedings of the National Academy of Sciences* **102**, 17907 (2005).

[9] A. J. Gellman, Imaging of Acetylene Heterocyclization Sites on the Sulfided Palladium(111) Surface, *Langmuir* **8**, 534 (1992).

[10] J. G. Kushmerick, S. A. Kandel, P. Han, J. A. Johnson, and P. S. Weiss, Atomic-Scale Insights into Hydrodesulfurization, *Journal of Physical Chemistry B* **104**, 2980 (2000).

[11] W. Eberhardt, F. Greuter, and E. W. Plummer, Bonding of H to Ni, Pd, and Pt Surfaces, *Physical Review Letters* **46**, 1085 (1981).

[12] J. H. Ferris, J. G. Kushmerick, J. A. Johnson, M. G. Y. Youngquist, R. B. Kessinger, H. F.Kingsbury, and P. S. Weiss, Design, Operation, and Housing of an Ultrastable, Low Temperature, Ultrahigh Vacuum Scanning Tunneling Microscope, *Review of Science Instruments* **69**, 2691 (1998).

[13] M. K. Rose, A. Borg, J. C. Dunphy, T. Mitsui, D. F. Ogletree, and M. Salmeron, Chemisorption of Atomic Oxygen on Pd(111) Studied by STM, *Surface Science* **561**, 69 (2004).

[14] M. K. Rose, A. Borg, T. Mitsui, D. F. Ogletree, and M. Salmeron, Subsurface Impurities in Pd(111) Studied by Scanning Tunneling Microscopy, *Journal of Chemical Physics* **115**, 10927 (2001).

[15] M. Gsell, P. Jakob, and P. Varga, STM and STS of Bulk Electron Scattering by Subsurface Objects, *Journal of Electron Spectroscopy and Related Phenomena* **109**, 71 (2000).

[16] G. Binnig, K. Frank, H. Fuchs, N. Garcia, B. Reihl, H. Rohrer, F. Salvan, and A. Williams, Tunneling Spectroscopy and Inverse Photoemission: Image and Field States, *Physical Review Letters* **55**, 991 (1995).

[17] R. J. Hamers, in *Scanning Tunneling Microscopy I* (H.-J. Guntherodt and R. Wiesendanger), Springer Series in Surface Science, Vol. 20, p. 83. Springer, Berlin, 1992.

[18] Y. Hasegawa and P. Avouris, Direct Observation of Standing Wave Formation at Surface Steps Using Scanning Tunneling Spectroscopy, *Physical Review Letters* **71**, 1071 (1993).

[19] M. F. Crommie, C. P. Lutz, and D. M. Eigler, Imaging Standing Waves in a Two-Dimensional Electron Gas, *Nature* **363**, 524 (1993).

[20] M. F. Crommie, C. P. Lutz, and D. M. Eigler, Spectroscopy of a Single Adsorbed Atom, *Physical Review B* **48**, 2851 (1993).

[21] S. L. Hulbert, P. D. Johnson, and M. Weinert, High-Resolution Inverse-Photoemission Study of the Pd(111) Surface, *Physical Review B* **34**, 3670 (1986).

[22] P. K. Hansma, *Tunneling Spectroscopy: Capabilities, Applications, and New Techniques*, Plenum, New York, 1982.

[23] C.-H. Hsu, M. El-Batanouny, and K. M. Martini, Dynamics of the Clean and Hydrogen Covered Pd(111) Surface, *Journal of Electron Spectroscopy and Related Phenomena* **54**, 353 (1990).

[24] D. L. Lynch, S. W. Rick, M. A. Gomez, B. W. Spath, J. D. Doll, and L. R. Pratt, Spectroscopic Studies of Surface and Subsurface Hydrogen/metal Systems, *Journal of Chemical Physics* **97**, 5177 (1992).

[25] H. W. Yeom, S. Takeda, E. Rotenberg, and S. Hasegawa, Instability and Charge Density Wave of Metallic Quantum Chains on a Silicon Surface, *Physical Review Letters* **82**, 4898 (1999).

[26] Y.-N. Hwang, S.-H. Park, and D. Kim, Size-Dependent Surface Phonon Mode of CdSe Quantum Dots, *Physical Review B* **59**, 7285 (1999).

[27] J. Szeftel, Surface Phonon Dispersion, Using Electron Energy Loss Spectroscopy, *Surface Science* **152**, 797 (1985).

[28] N. V. Richardson and J. C. Campuzano, The Adsorption of Thiophene on a Cu(111) Surface, *Vacuum* **31**, 449 (1981).

[29] G. R. Schoolf, R. E. Preston, and J. B. Benziger, Adsorption and Desulfurization of Thiophene on Nickel(111), *Langmuir* **1**, 313 (1985).

[30] J. Stohr, J. L. Gland, E. B. Kollin, R. J. Koestner, A. L. Johnson, and E. L. Muetterties, Desulfurization and Structural Transformation of Thiophene on the Pt(111) Surface, *Physical Review Letters* **53**, 2161 (1984).

[31] E. R. Frank, X. X. Chen, and R. J. Hamers, Direct Observation of Oriented Molecular Adsorption at Step Edges: a Cryogenic Scanning Tunneling Microscopy Study, *Surface Science* **334**, 709 (1995).

[32] T. E. Caldwell and D. P. Land, Desulfurization, Deoxygenation and Denitrogenation of Heterocycles by a Palladium Surface: a Mechanistic Study of Thiophene, Furan and Pyrrole on Pd(111) Using Laser-Induced Thermal Desorption with Fourier-Transform Mass Spectrometry, *Polyhedron* **16**, 3197 (1997).

[33] X. X. Chen, E. R. Frank, and R. J. Hamers, Spatially and Rotationally Oriented Adsorption of Molecular Adsorbates on Ag(111) Investigated Using Cryogenic Scanning Tunneling Microscopy, *Journal of Vacuum Science and Technology B* **14**, 1136 (1996).

[34] D. N. Futaba and S. Chiang, Calculations of Scanning Tunneling Microscopic Images of Benzene on Pt(111) and Pd(111), and Thiophene on Pd(111), *Japanese Journal of Applied Physics* **38**, 3809 (1999).

[35] A. Loui and S. Chiang, Investigation of Furan on Vicinal Pd(1 1 1) by Scanning Tunneling Microscopy, *Applied Surface Science* **237**, 555 (2004).

[36] E. C. H. Sykes, B. A. Mantooth, P. Han, Z. J. Donhauser, and P. S. Weiss, Substrate-Mediated Intermolecular Interactions: A Quantitative Single Molecule Analysis, *Journal of the American Chemical Society* **127**, 7255 (2005).

[37] R. Smoluchowski, Anisotropy of the Electronic Work Function of Metals, *Physical Review* **60**, 661 (1941).

[38] M. J. Aroney, H. K. Lee, and R. J. W. Lefevre, The Conformation of 2,2'-bithienyl in Solution, *Australian Journal of Chemistry* **25**, 1561 (1972).

[39] S. J. Stranick, M. M. Kamma, P. S. Weiss, Atomic-Scale Dynamics of a Two-Dimensional Gas-Solid Interface, *Science* **266**, 99 (1994).

[40] S. Terada, T. Yokoyama, M. Sakano, A. Imanish, Y. Kitajima, M, Kiguchi, Y. Okamoto, and T. Ohta, Thiophene Adsorption on Pd(111) and Pd(100) Surfaces Studied by Total-Reflection S K-Edge X-Ray Absorption Fine-Structure Spectroscopy, *Surface Science* **414**, 107 (1998).

[41] P. Sautet and M.-L. Bocquet, Shape of Molecular Adsorbates in STM Images: A Theoretical Study of Benzene on Pt(111), *Physical Review B* **53**, 4910 (1995).

[42] P. S. Weiss and D. M. Eigler, Site Dependence of the Apparent Shape of a Molecule in Scanning Tunneling Micoscope Images: Benzene on Pt{111}, *Physical Review Letters* **71**, 3139 (1993).

[43] M. M. Kamna, S. J. Stranick, and P. S. Weiss, Imaging Substrate-Mediated Interactions, *Israel Journal of Chemistry* **36**, 59 (1996).

[44] R. P. Feynman, There's Plenty of Room at the Bottom, *Engineering and Science* **23**, 22 (1960).

[45] D. Eigler and E. K. Schweitzer, Positioning Single Atoms with a Scanning Tunnelling Microscope, *Nature* **344**, 524 (1990).

[46] B. J. Mclntyre, M. Salmeron, and G. A. Somorjai, Nanocatalysis by the Tip of a Scanning Tunneling Microscope Operating Inside a Reactor Cell, *Science* **265**, 1415 (1994).

[47] B. C. Stipe, M. A. Rezaei, and W. Ho, Inducing and Viewing the Rotational Motion of a Single Molecule, *Science* **279**, 1907 (1998).

[48] B. C. Stipe, M. A. Rezaei, and W. Ho, Coupling of Vibrational Excitation to the Rotational Motion of a Single Adsorbed Molecule, *Physical Review Letters* **81**, 1263 (1998).

[49] H. J. Lee and W. Ho, Single-Bond Formation and Characterization with a Scanning Tunneling Microscope, *Science* **286**, 1719 (1999).

[50] J. I. Pascual, N. Lorente, Z. Song, H. Conrad, and H.-P. Rust, Selectivity in Vibrationally Mediated Single-Molecule Chemistry, *Nature* **423**, 525 (2003).

[51] G. P. Salam, M. Persson, and R. E. Palmer, Possibility of Coherent Multiple Excitation in Atom Transfer with a Scanning Tunneling Microscope, *Physical Review B* **49**, 10655 (1994).

[52] T. Komeda, Y. Kim, Maki Kawai, B. N. Persson, and H. Ueba, Lateral Hopping of Molecules Induced by Excitation of Internal Vibration Mode, *Science* **295**, 2055 (2002).

Vita

Rong Zhang

Education

2004-2008: The Pennsylvania State University, University Park, PA
M.S. in Chemistry, May 2008
Thesis Advisor: Professor Paul Weiss

1999-2004: University of Science and Technology of China, Hefei, P.R.China
B.S. in Chemical Physics, July 2004
Thesis Advisor: Yi Xie

Professional and Teaching Experience

2005-2008: Research Assistant, Department of Chemistry,
The Pennsylvania State university

2005-2006: Teaching Assistant, Department of Chemistry
The Pennsylvania State University

2002-2004: Research Assistant, Department of Chemical Physics
University of Science and Technology of China